

Quasi-two-dimensional conducting layer on TiO₂ (110) introduced by sputtering as a template for resistive switching

M. Rogala, Z. Klusek, C. Rodenbücher, R. Waser, and K. Szot

Citation: [Appl. Phys. Lett.](#) **102**, 131604 (2013); doi: 10.1063/1.4801437

View online: <http://dx.doi.org/10.1063/1.4801437>

View Table of Contents: <http://apl.aip.org/resource/1/APPLAB/v102/i13>

Published by the [American Institute of Physics](#).

Additional information on Appl. Phys. Lett.

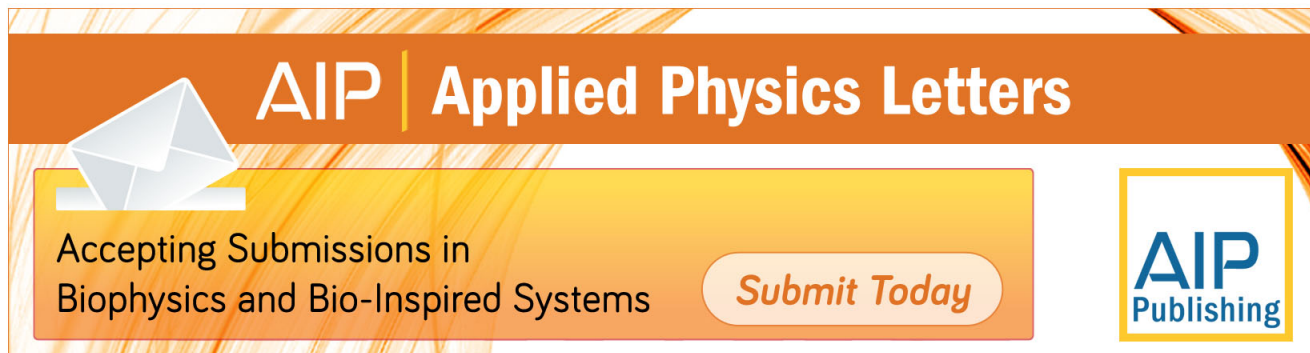
Journal Homepage: <http://apl.aip.org/>

Journal Information: http://apl.aip.org/about/about_the_journal

Top downloads: http://apl.aip.org/features/most_downloaded

Information for Authors: <http://apl.aip.org/authors>

ADVERTISEMENT

The advertisement banner features a background of orange and yellow diagonal stripes. At the top, the "AIP | Applied Physics Letters" logo is displayed in white. Below the logo, on the left, is a white icon of an envelope. To the right of the envelope, the text "Accepting Submissions in Biophysics and Bio-Inspired Systems" is written in black. Further right, a white button with the text "Submit Today" in orange is visible. On the far right, the "AIP Publishing" logo is shown in a yellow-bordered box.

AIP | Applied Physics Letters

Accepting Submissions in
Biophysics and Bio-Inspired Systems

Submit Today

AIP
Publishing

Quasi-two-dimensional conducting layer on TiO₂ (110) introduced by sputtering as a template for resistive switching

M. Rogala,^{1,2,a)} Z. Klusek,² C. Rodenbücher,¹ R. Waser,^{1,3} and K. Szot^{1,4}

¹Peter Grünberg Institute and JARA-FIT, Forschungszentrum Jülich, 52425 Jülich, Germany

²Division of Physics and Technology of Nanometre Structures, Faculty of Physics and Applied Informatics, University of Lodz, 90-236 Lodz, Pomorska 149/153, Poland

³IWE 2 and JARA-FIT, RWTH Aachen University, 52056 Aachen, Germany

⁴University of Silesia, Institute of Physics, 40-007 Katowice, Poland

(Received 25 February 2013; accepted 27 March 2013; published online 5 April 2013)

The insulator-to-metal transformation in the surface layer of TiO₂ (110) induced by the Ar⁺ ion sputtering process is analyzed on the nanoscale. Local conductivity atomic force microscopy and photoelectron spectroscopy allow the changes in the valence of the Ti ions in the surface layer to be linked to the formation of its grain-like structure. The investigation of the cleavage plane of the crystal allowed us to estimate the thickness of the quasi-two-dimensional conducting layer generated by ion bombardment as 30 nm. The conducting layer is a template where the resistive switching of each single grain can be carried out. © 2013 AIP Publishing LLC. [<http://dx.doi.org/10.1063/1.4801437>]

Resistive switching (RS) processes in TiO₂ (Refs. 1–3) are highly promising for application to redox-based resistive random-access memory (ReRAM).^{4–7} However, the exact mechanism responsible for changing the electrical conductivity in this material is still under debate.¹ The optimum starting point for a consideration of the origin of RS in TiO₂ is the perfect material, which in this case means a single crystal. However, the high initial resistivity of pristine rutile TiO₂ should be reduced before any RS experiment. This forming step can be achieved by the influence of either a chemical or electrical gradient or by electron/ion irradiation. The most common way of reducing the crystal resistivity is vacuum annealing. However, this process is not optimal for electronic applications because it takes place in the whole volume of the sample. In contrast, electron and ion irradiations are a selective way of TiO₂ modification. Especially Ar⁺ ion sputtering is an effective process which may lead to the creation of a quasi-two-dimensional (quasi-2D) metallic layer on the surfaces of insulating binary and ternary transition-metal oxide substrates^{8–11} and, as previously shown for SrTiO₃,¹² can prepare the surface for further RS. The nature of the metal-insulator transition (MIT) induced in these materials by an ion bombardment process has previously been investigated, regarding the changes in oxygen stoichiometry and macroscopic surface conductivity.^{8,9,13,14} However, in the literature, there is no description of the transformation from band insulator to metallic conductor at the nanoscale, based on the results of local conductivity atomic force microscopy (LC-AFM). In this letter, we analyze this essential aspect of MIT in the surface layer of TiO₂ (110) single crystals by investigations of nanoscale conductivity distribution in-plane of the surface layer at various temperatures. Additionally, our out-of-plane measurements enable us to estimate the depth of changes introduced into the crystal by the ion sputtering process. We show that the quasi-2D surface layer, which we prepare by ion bombardment, can work as a template for nanoscale RS, and the resolution and the mechanism of switching are also strictly

connected to the surface substructure that we characterized. We use scanning probe microscopic techniques (AFM/LC-AFM), both with X-ray and UV photoelectron spectroscopy (XPS/UPS), to describe the complexity of transformations that occur in the electronic structure, crystal geometry, and local conductivity.

In our study, commercially available TiO₂ (110) rutile crystals were used. After initially removing the physisorbates from the surface by thermal treatment at 300 °C under vacuum conditions, the stoichiometry, electronic structure, and crystal geometry show properties typical of a perfect TiO₂ (110) surface as described in the literature.¹⁵ All Ti ions had a 4+ oxidation state, there were no occupied electron states in the band gap, and the low energy electron diffraction showed a clear 1 × 1 pattern. Next, such pristine TiO₂ substrates were repeatedly sputtered with Ar⁺ ions of 2 keV energy and current density close to 10 μA/cm². The influence of every sputtering step (1 min) on the physical properties of the surface layer was controlled by XPS and UPS, and the modification of surface resistivity was analyzed by LC-AFM. The sputtering process was continued until the steady state was reached in surface composition and resistivity, and no significant changes were achieved by extending the treatment time.

During the Ar⁺ sputtering process, the selective removal of oxygen leads to a progressive reduction of part of the Ti⁴⁺ ions to the 3+ or 2+ oxidation state, which can be identified as a kind of a redox reaction. As a result, a continuum of occupied Ti3d electrons starts to appear in the band gap.^{16–19} This process leads to the transformation of the material from intrinsic semiconductor to n-type semiconductor and finally to semi-metal. The binding energies of core-level electrons resulting from Ti³⁺ and Ti²⁺ ions differ from those obtained from Ti⁴⁺ (approximately 1.8 eV and 3.8 eV, respectively) and can be distinguished by XPS. Figure 1(a) shows the composition of the surface layer with respect to the percentage content of Ti⁴⁺, Ti³⁺, and Ti²⁺ during the sputtering process (estimated from XPS results). From the beginning, reduction processes from Ti⁴⁺ to Ti³⁺-type structures occurred, which are more likely than reduction to Ti²⁺

^{a)} Author to whom correspondence should be addressed. Electronic mail: rogala@uni.lodz.pl

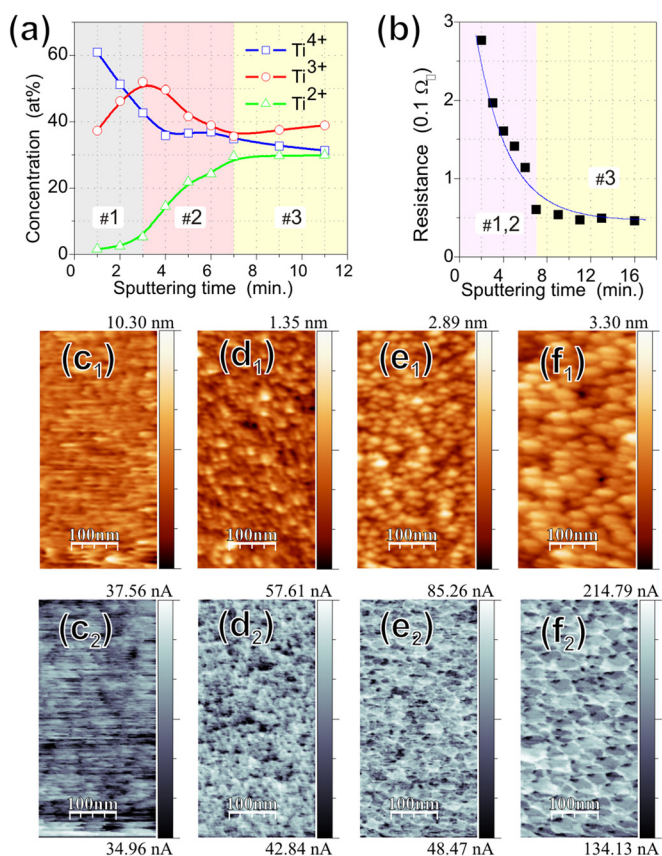


FIG. 1. Comparison of TiO₂ (110) surface changes with increasing time of sputtering. (a) The quantitative changes in the representation of different Ti ions in the surface layer (analyzed in XPS measurement). (b) The changes in the resistance (in $\Omega/\mu\text{m}^2$) of the surface (based on data collected using LC-AFM). (c₁)–(f₁) The topography and (c₂)–(f₂) local conductivity images (LC-AFM; $250 \times 500 \text{ nm}^2$; sample-tip polarization 0.1 V) of the surface after 2, 3, 5, and 9 min, respectively, of sputtering.

(region #1 in Fig. 1(a)). However, when the Ti³⁺ content is close to 50%, the reduction to Ti²⁺ becomes visible, and at the same time the Ti⁴⁺ ion content approaches a constant value (region #2). Moreover, we are constantly dealing with the removal of the surface material and sputtering of the deeper regions of the sample. Consequently, after approximately 7–8 min of sputtering, the surface and subsurface stoichiometry, sputtering rate, and reduction processes between each type of ion structure approach equilibrium, and the composition-to-time dependence reaches a constant level (region #3). This macroscopic behavior seems to correspond to the theoretical model proposed by Hashimoto *et al.*^{13,14} However, we should bear in mind that the reduction of TiO₂ with only Ti⁴⁺ ions to a system of lower oxidation states is not based simply on a transformation to a Ti₂O₃ phase and later to a TiO phase but consists in the appearance of various structural defects and substoichiometric (Ti_nO_{2n-1}) phases¹ and leads to a strong modification of the topography and conductivity of the surface. This is confirmed by our LC-AFM results. The topography after long-time sputtering shows a structure composed of distinct grains which fill all of the available surface space. The in-plane dimensions of the grains increase significantly with the time of sputtering (approximately 25 nm–50 nm), which is presented in the set of images (Figures 1(c₁)–1(f₂)). In the in-plane conductivity (Figs. 1(c₂)–1(f₂)) which is essentially

inhomogeneous, we can distinguish well-conducting grains, their boundaries (which are even more conductive), and rare, less conductive points.

The compositional changes from the beginning of sputtering described above are accompanied by a gradual decrease of surface resistivity, as shown in Figure 1(b). The data presented are calculated on the basis of LC-AFM conductivity maps collected on the TiO₂ surface after each step of sputtering and expressed in the resistivity of the square of area of $1 \mu\text{m}^2$. It can be seen that significant changes in average conductivity occur up to the 7–9th minute of the sputtering process (region #1, 2 in Fig. 1(b)) while, after this time (when the surface composition is nearly constant with respect to Ti⁴⁺, Ti³⁺, and Ti²⁺ ions), the conductivity of the system is close to the equilibrium state (region #3). It is important to note that the process of changes in composition and surface resistivity does not fully correspond to the process of transformation in surface morphology. As shown in the set of topography images (Figures 1(c₁)–1(f₁)) and corresponding local conductivity images (Figs. 1(c₂)–1(f₂)), such a process starts from distinct amorphization, and with time the grain dimensions gradually increase up to the limit, which is close to 50 nm in diameter. However, this limit is reached at approximately the 16th min of sputtering, which is long after reaching equilibrium in surface composition and resistivity (at approximately the 8th minute of sputtering—taking into account the values of energy and current density previously given). This suggests that even after reaching the limit of reduction of the surface layer we are dealing with significant processes of reorganization of the crystallographic structure of the Ti-O system, which can be considered as a nanoscale transformation to new oxygen-deficient (compared to TiO₂) phases.^{20,21} Comparable transformations have previously been reported for rutile irradiated by electrons, where sufficiently large beam energies and current densities led to the appearance of TiO crystallites on the investigated surfaces.^{22,23} The observed grain-forming process may be associated with a well-known phenomenon of self-organization of the surface due to ion sputtering.^{24,25} However, in this case it is a direct consequence of the surface reduction (preferential removal of oxygen) and corresponding transformations.

The complexity of the surface layer transformation can also be observed based on an analysis of the electrical properties of the surface in the early stages of the sputtering process. For a slightly sputtered surface (1 min) we collected numerous LC-AFM maps of surface conductance at various temperatures, and on this basis we calculated the average surface resistances (expressed in the resistivity of $1 \mu\text{m}^2$ square), which are shown in Figure 2(a) (red circles). Below 200 °C, the slightly sputtered TiO₂ surface behaves like a semiconductor (linear dependence on the Arrhenius plot), but above this temperature the dependence becomes nearly flat, corresponding to the metallic properties of the material. The observed metal-insulator transition was also previously reported for the TiO₂ surface reduced by annealing in UHV.¹ Such a transition may be related to the presence of the Ti₂O₃ phase on the surface, which is characterized by MIT in a similar temperature range. However, such behavior is not observed after exposure of the surface to the oxygen

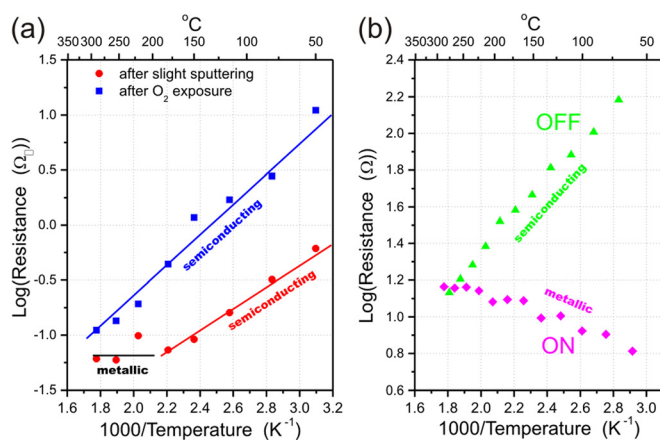


FIG. 2. (a) The thermal dependence of the resistance of the TiO₂ crystal surface after slight ion sputtering (1 min) and after further oxygen exposure (dose = 10⁶ L) (based on LC-AFM measurements). (b) The thermal dependence of the resistance of the grain in the OFF and ON state.

atmosphere (blue square dependence in Figure 2(a)). After this process, the resistivity of the surface is about ten times larger, and in the whole range of investigated temperatures the material behaves like a semiconductor with slightly larger thermal activation energy than previously. On the other hand, the surface conductivity is not reduced completely. This confirmed that even a slight sputtering process can lead to the appearance of more stable nonstoichiometric Ti-O phases on the TiO₂ surface, which in contrast to oxygen vacancies cannot be removed during oxidation. It should be noted that in the case of the surface of the single crystal, the described electrical characterization is the most appropriate way of studying and identifying such phases because the preparation methods necessary to perform complementary investigations (e.g., high-resolution transmission electron microscopy (HRTEM)) will simultaneously lead to considerable modification of the sample. Moreover, it was shown that HRTEM measurement can itself provide noticeable changes in the structure of transition metal oxides.^{26,27}

As already mentioned, after long sputtering processes on the surface of oxide crystals we are dealing with a well-conducting quasi-2D layer, which was described previously by Reagor and Butko for SrTiO₃.⁸ However, it is important to estimate the real thickness of a structure generated in this way. To do so we conducted a specific experiment in which after 16 min of sputtering the crystal was cleft *ex situ* perpendicular to the surface and later investigated in the plane of cleavage with LC-AFM (Figs. 3(a)–3(c)). The thickness of the well-conducting layer can be estimated to be about 30 nm based on the local conductivity images and their cross sections from Figures 3(a) and 3(b). A well-conducting quasi-2D layer can be observed there as a bright (high-conductivity) stripe in the middle of the image. The left part of the image, where the electrical conductivity is weaker, is related to the primary (sputtered) surface, whose conductivity was also high, but decreased due to of physisorption and chemisorption²⁸ at the time of the splitting process. The crystal was prepared and split *ex situ*, while the LC-AFM measurements were conducted directly after the splitting process, which decreased the contamination effect of the cleavage plane. The thickness of the well-conducting layer obtained is

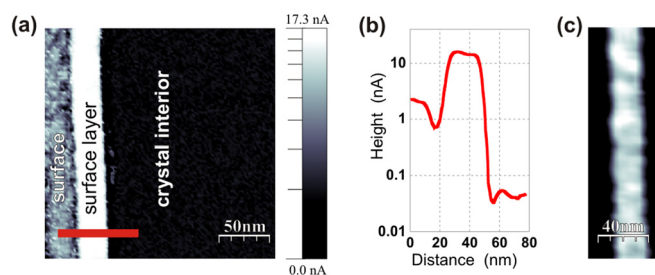


FIG. 3. LC-AFM measurements in the cleavage plane of previously sputtered TiO₂: (a) local conductivity image (225 × 225 nm²; sample-tip polarization 3.0 V); (b) cross sections along the marked line; (c) magnification of the region of high-conductivity surface layer (60 × 180 nm²; polarization 2.0 V).

slightly larger than the ion penetration depth described in the literature^{29,30} during the sputtering process, which should not be larger than 10 nm. In that case, we are dealing with a more complex transformation of a reduced (by sputtering) surface region into new Ti-O phases. Our result is closer to the results presented by Kan *et al.*,¹⁰ where they describe the 20 nm deep surface modification which is the result of Ar⁺ sputtering of SrTiO₃. It should also be noted that in the described grain-like structure (which forms the surface layer) the sets of the closely packed well-conducting columns can be identified (as can be seen in the magnification of the surface layer presented in Figure 3(c)). Similar structures in the shape of cones consisting of nonstoichiometric Ti-O phases were observed previously by Kwon *et al.*⁷ for the TiO₂ after electroreduction.

The electrical properties of the grains produced in the sputtering process can be modified by electrical stimulation by the LC-AFM tip. With increasing the tip-grain polarization, we obtained the resistive switching effect. However, the change of local conductivity is observed on the whole area of the grain, regardless of the specific position of the tip over the grain during the switching procedure. In Figure 4(a), we show a selected grain (marked by a dashed line) in two easily distinguishable states of high (OFF) and low (ON) resistivity. The switching between states was induced by applying +5 V and −5 V to the tip. The analysis of the thermal dependence of grain resistivity in the OFF and ON state (shown in Fig. 2(b)) indicates that the observed RS consists in a transformation between the semiconducting and metallic character of material conductivity. Therefore the observed changes in conductivity are similar in their nature to the oxidation-induced transformations of a briefly sputtered surface (Fig. 2(a)). It should be noted that RS was already observed on the grains at their early formation stages (after 3–4 min sputtering), when their dimensions approach 20 nm.

The optimal RS effect was achieved after exposure of the surface to the oxygen dose (>10⁵ L). The XPS results (not shown) indicate that under such conditions the concentration of Ti⁴⁺ ions increases at the expense of ions on the lower oxidation states. Additionally, the maps of the local conductivity confirm that the intergranular areas, which before oxygen exposure are more conductive than grains and after exposure become less conductive (compare Figs. 1(f₂) and 4(a)), are more susceptible to oxidation. This leads to the hypothesis that during RS we are not dealing with changes in the resistivity of the grain but with the changes in the

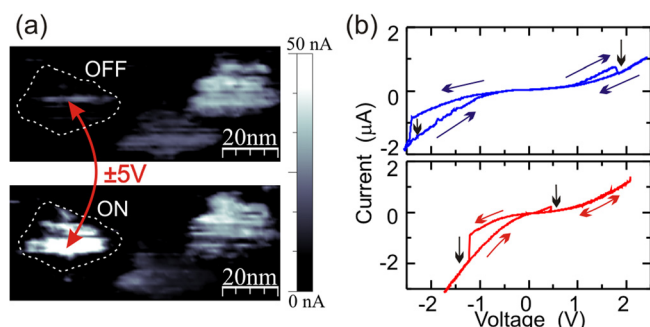


FIG. 4. The resistivity switching of a single grain on the surface layer of TiO_2 after 3 min of sputtering. (a) Local conductivity images (LC-AFM; $100 \times 40 \text{ nm}^2$; sample-tip polarization 20 mV) of the grain in the high (OFF) and low (ON) resistivity state (top and bottom part). (b) $I(V)$ switching curves for two sample grains.

resistivity of its connections to the other parts of the sputtered surface layer. The oxygen delivered to the intergranular areas can participate in the electrically induced modification of the resistivity of the surroundings of the grain, which results in the RS observed for the selected grain. It should be noted that the ease of oxidation of the intergranular areas suggests their amorphous structure in comparison with grains formed in a more stable nanocrystalline form.

Observed bipolar RS shows that the sputtered TiO_2 surface is in fact a template ready for information storage, where the storage density is determined by the dimensions of the grains. The investigation of the grain population indicate that RS occurred in the range of a few V and is characterized by the $I(V)$ curves oscillating between the two presented in Figure 4(b). Although bipolar switching is observed, the individual grain voltage required for the transition between the states and the ratio of resistances in these states can vary.

In conclusion, we show that self-organization of the TiO_2 (110) surface layer during the Ar^+ sputtering process is a promising way of producing a template for high-resolution resistive switching on the nanoscale. We concentrated on the description of the complexity of the sputtering-induced transformation of the crystal regarding the changes occurring in topography (morphology), stoichiometry, electronic structure, and electric transport. We were able to analyze the changes in conductivity both in- and out-of-plane of the crystal surface layer. The presented results prove that from the beginning of the sputtering process we are dealing with a transformation in the morphology and heterogeneous distribution of surface conductivity, which can be correlated with the decrease in the oxygen stoichiometry and oxidation state of Ti. However, such changes are also observed for some of the prolonged sputtering period, when a balance of surface stoichiometry, oxidation state of Ti and conductance is already established. At the early stages of the process, we find (by LC-AFM measurements at various temperatures) the electrical signature of the presence of the Ti_2O_3 phase in the sputtered layer. As a consequence of increasing time of Ar^+ ion bombardment, the surface adopts a self-organized grain-like structure with grain dimensions increasing (with sputtering time) up to 50 nm. Based on the investigations of the cleavage plane of the previously sputtered crystal, we estimated the thickness of such a quasi-2D layer as 30 nm.

The electrical conductivity of the layer displays a very sharp boundary. Our results show that on the surface of TiO_2 crystal the Ar^+ ion sputtering process produces a self-organized template for resistive switching in which each of the grains can be individually addressed (electrically) and switched between the semiconducting (OFF) and metallic (ON) state. The observed phenomenon has a unique potential for use in a very well-located data storage concept.

The authors would like to thank Professor U. Diebold for helpful discussions concerning the presented results. The work was co-financed by the University of Lodz (Grant supporting young scientists) and the Deutsche Forschungsgemeinschaft (SFB 917).

- ¹K. Szot, M. Rogala, W. Speier, Z. Klusek, A. Besmehn, and R. Waser, *Nanotechnology* **22**, 254001 (2011).
- ²J. R. Jameson, Y. Fukuzumi, Z. Wang, P. Griffin, K. Tsunoda, G. I. Meijer, and Y. Nishi, *Appl. Phys. Lett.* **91**, 112101 (2007).
- ³M. H. Lee, K. M. Kim, G. H. Kim, J. Y. Seok, S. J. Song, J. H. Yoon, and C. S. Hwang, *Appl. Phys. Lett.* **96**, 152909 (2010).
- ⁴D. B. Strukov, G. S. Snider, D. R. Stewart, and R. S. Williams, *Nature (London)* **453**, 80 (2008).
- ⁵R. Waser and M. Aono, *Nat. Mater.* **6**, 833 (2007).
- ⁶B. J. Choi, D. S. Jeong, S. K. Kim, C. Rohde, S. Choi, J. H. Oh, H. J. Kim, C. S. Hwang, K. Szot, R. Waser, B. Reichenberg, and S. Tiedke, *J. Appl. Phys.* **98**, 033715 (2005).
- ⁷D.-H. Kwon, K. M. Kim, J. H. Jang, J. M. Jeon, M. H. Lee, G. H. Kim, X.-S. Li, G.-S. Park, B. Lee, S. Han, M. Kim, and C. S. Hwang, *Nat. Nanotechnol.* **5**, 148 (2010).
- ⁸D. W. Reagor and V. Y. Butko, *Nat. Mater.* **4**, 593 (2005).
- ⁹B. Psiuk, J. Szade, M. Pilch, and K. Szot, *Vacuum* **83**(Suppl. 1), S69 (2009).
- ¹⁰D. Kan, T. Terashima, R. Kanda, A. Masuno, K. Tanaka, S. Chu, H. Kan, A. Ishizumi, Y. Kanemitsu, Y. Shimakawa, and M. Takano, *Nat. Mater.* **4**, 816 (2005).
- ¹¹J. Kubacki, A. Molak, M. Rogala, C. Rodenbücher, and K. Szot, *Surf. Sci.* **606**, 1252 (2012).
- ¹²H. Gross and S. Oh, *Appl. Phys. Lett.* **99**, 092105 (2011).
- ¹³S. Hashimoto, A. Tanaka, A. Murata, and T. Sakurada, *Surf. Sci.* **556**, 22 (2004).
- ¹⁴S. Hashimoto and A. Tanaka, *Surf. Interface Anal.* **34**, 262 (2002).
- ¹⁵U. Diebold, *Surf. Sci. Rep.* **48**, 53 (2003).
- ¹⁶V. E. Henrich, G. Dresselhaus, and H. J. Zeiger, *Phys. Rev. Lett.* **36**, 1335 (1976).
- ¹⁷C. M. Yim, C. L. Pang, and G. Thornton, *Phys. Rev. Lett.* **104**, 036806 (2010).
- ¹⁸P. Krüger, J. Jupille, S. Bourgeois, B. Domenichini, A. Verdini, L. Floreano, and A. Morgante, *Phys. Rev. Lett.* **108**, 126803 (2012).
- ¹⁹K. Mitsuhashi, H. Okumura, A. Visikovskiy, M. Takizawa, and Y. Kido, *J. Chem. Phys.* **136**, 124707 (2012).
- ²⁰L. A. Bursill, B. G. Hyde, O. Terasaki, and D. Watanabe, *Philos. Mag.* **20**, 347 (1969).
- ²¹C. R. A. Catlow, *Nonstoichiometric Oxides* (Academic Press, New York, 1981).
- ²²M. McCartney and D. J. Smith, *Surf. Sci.* **250**, 169 (1991).
- ²³M. McCartney, P. Crozier, J. Weiss, and D. J. Smith, *Vacuum* **42**, 301 (1991).
- ²⁴S. Facsko, T. Dekorsy, C. Koerdts, C. Trappe, H. Kurz, A. Vogt, and H. L. Hartnagel, *Science* **285**, 1551 (1999).
- ²⁵A. Cuenat, H. George, K.-C. Chang, J. Blakely, and M. Aziz, *Adv. Mater.* **17**, 2845 (2005).
- ²⁶D. J. Smith and L. Bursill, *Ultramicroscopy* **17**, 387 (1985).
- ²⁷D. J. Smith, M. McCartney, and L. Bursill, *Ultramicroscopy* **23**, 299 (1987).
- ²⁸F. Peter, A. Rudiger, R. Dittmann, R. Waser, K. Szot, B. Reichenberg, and K. Prume, *Appl. Phys. Lett.* **87**, 082901 (2005).
- ²⁹M. Wolff and J. W. Schultz, *Surf. Interface Anal.* **12**, 93 (1988).
- ³⁰*Low Energy Ion-Surface Interactions*, edited by J. W. Rabalais (Wiley, Chichester, 1994), Chap. 9.